

# A Scalable Solar Antenna for Autonomous Integrated Wireless Sensor Nodes

Terence Wu, *Student Member, IEEE*, Ronglin Li, *Senior Member, IEEE*, and Manos. M. Tentzeris, *Fellow, IEEE*

**Abstract**—A novel scalable low-profile omnidirectional antenna that can be integrated underneath a solar panel is presented. The topology alleviates the effect of solar panel to the antenna while achieving a monopole-like radiation performance above a ground plane. A  $72 \times 72 \times 11.5 \text{ mm}^3$  solar antenna 3-D structure operating around 2.4 GHz demonstrates the potential of the presented configuration for the implementation of autonomous integrated wireless sensors nodes.

**Index Terms**—3-D RF modules, autonomous modules, omnidirectional antenna, solar antenna, solar panel, wireless sensor nodes.

## I. INTRODUCTION

WIRELESS sensor networks (WSNs) are composed of a large number of sensor nodes densely deployed within a given area. Each of these sensors nodes has the capability of processing data and transmitting only the required information across the network [1]. These architectures provide better network reliability and easier deployment than traditional tethered sensor systems. The ease of deployment allows the implementation of cheap and pervasive networks that can impact a range of applications from medical monitoring, target/hazard detection, to industrial/automotive control [2]–[4]. Existing deployments include climate monitoring in botanical gardens and structural monitoring of bridges [5], [6], and applications such as forest fire detection, wireless building security systems, and smart roads may be available in the years to come [7]–[9].

Node reliability is a major challenge for WSN quality of service that could drastically increase the cost of maintenance after deployment [10]. Node malfunction can be caused by energy shortage, mechanical failure, sensor relocation, etc. To eliminate issues due to energy shortage, power harvesting mechanisms have been introduced to support the power consumption of every individual node [11]. Currently, solar panels harvest the largest reported amount of energy per area in outdoor environments, and many designs have integrated them with sensor nodes' power management system [12]. Monopole antennas are

currently used in the majority of WSN nodes because of their simplicity and quasi-isotropic radiation. However, monopoles positioned perpendicularly to the ground are highly susceptible to mechanical damages such as being rolled over by a car or run over by an animal [13]. Such an event leads to wireless link failure of the node. This type of failure is currently reduced by deploying wireless sensor nodes in locations where cars or animals cannot move on top of them or extreme environmental conditions cannot displace them. Nevertheless, to realize truly ubiquitous and easy-to-deploy WSNs, it is necessary to come up with a rugged antenna that offers structural durability and omnidirectional communication features. This antenna needs to be fully compatible with the solar panels that supply the sensors' power while featuring a similar radiation performance to a monopole near grounding or shielding conductive planes.

Several authors have investigated designs and methods of integrating solar cells with antennas [14]–[17]. However, most of them are intended for ground-to-air satellite applications where most of the radiation is directed toward the zenith of antennas [14]–[16]. A study in [17] indicated that typical solar panels behave as imperfect conductors in the RF frequency range. Due to power circuitry connecting several solar cells together, a solar panel becomes similar to a large RF ground that can potentially block or interfere with the transmitted RF signals of neighboring/underlying radiating elements.

Although numerous low-profile omnidirectional antennas have been introduced in the literature, such as the annular slot antenna (ASA) [18] and the monopolar patch [19]–[21], there has been no report on any integration with solar panels. An ASA, when placed underneath a solar panel, may have its radiation pattern distorted by a solar cell's power lines intersecting the slot because such a configuration is similar to placing a short circuit across the slot [22], [23]. Henze [17] introduced an omnidirectional solar antenna design by using an antenna topology similar to a monopolar patch as well as an ASA. However, the location of the power line intersecting the radiating solar cell was not addressed.

In terms of design scalability, both ASA and monopolar patch are frequency-dependent; their integration with different sizes of solar panels at different operating frequencies is a unique, specific design challenge of its own. Wu [24] introduced a method of generating an omnidirectional pattern by cutting multiple slots on the surface of a ground plane, placing solar cells at the nonslot region, and connecting the cells without crossing those slots. However, such a design requires dicing and placing several small solar panels around the slots, increasing the fabrication cost. An antenna topology that can coexist with an arbitrary solar panel size is desirable for reducing both the cost of the device as well as the cost of the integration.

Manuscript received March 02, 2011; revised April 11, 2011; accepted May 02, 2011. Date of publication May 12, 2011; date of current version May 31, 2011. This work was supported by the Federal Highway Administration under Agreement No. DTFH61-10-H-00004, the Overseas Distinguished Professor Program, and the IFC/SRC.

T. Wu and M. M. Tentzeris are with the School of Electrical and Computer Engineering, Georgia Institute of Technology, Atlanta, GA 30332 USA (e-mail: twu@ece.gatech.edu; etentze@ece.gatech.edu).

R. Li is with School of Electronic and Information Engineering, South China University of Technology, Guangzhou 510641, China (e-mail: lirl@scut.edu.cn).

Color versions of one or more of the figures in this letter are available online at <http://ieeexplore.ieee.org>.

Digital Object Identifier 10.1109/LAWP.2011.2152357

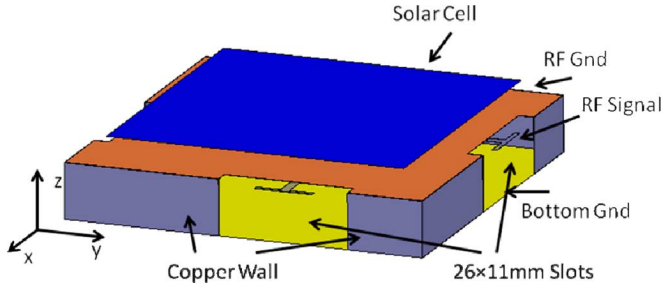


Fig. 1. Angular view of the structure showing the solar cell and the conductor layers.

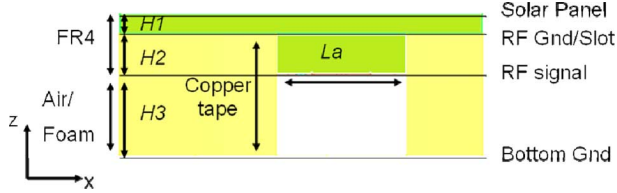


Fig. 2. Layer stackup of the solar antenna.

In this letter, a low-profile scalable topology that allows integration of an arbitrary-sized solar panel with an omnidirectional antenna is presented. The two major advantages of this typology are that it minimizes the effect of a solar cell on the antenna, and it is planar with nothing protruding the surface contrary to monopole radiators, thus being easy to analyze and package. As a proof of concept and without loss of generality, an antenna prototype hosting a  $6 \times 6 \text{ cm}^2$  solar panel is designed for 2.4-GHz applications. The radiation performance of the antenna above a finite ground plane is studied to demonstrate its radiation similarity with a standard monopole.

## II. ANTENNA DESIGN AND MEASUREMENT

### A. Design

The proposed four-layer integrated solar cell–antenna stackup is shown in Figs. 1 and 2. It consists of a three-layer 62-mil FR4 board ( $\epsilon_r = 4.65$ ,  $\tan \delta = 0.018$ ) and an air cavity supported by 1-cm-thick foam ( $\epsilon_r = 1$ ). The air cavity provides a low-loss medium for the RF signal line and the higher thickness needed. The top metal layer represents the solar panel. The second layer consists of a larger-area RF ground plane that aims at isolating the solar cell from the underlying RF signal layers and providing radiating slot openings cut on all four sides. The solar panel is separated from the RF ground layer so that the dc bias of the RF transceiver input/output is stable at various energy harvesting conditions. The third layer carries the RF signal to be coupled and radiated through the slots. The stackup is backed up by a bottom (layer 4) solid copper ground plane. To provide a better ground isolation and eliminate the parallel plate mode in the structure, copper tape is applied around the board to connect the RF ground to the bottom copper plane forming a cavity of four slot openings.

Fig. 3 gives the top view of the RF ground plane and the RF signal pattern in layers 2 and 3 of the FR4 board. Layers 1 and 4 are not shown due to their simplicity. Layer 1 is one

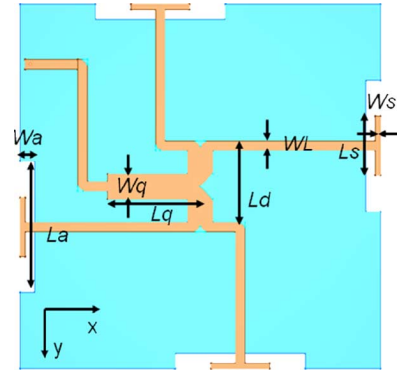


Fig. 3. RF signal and ground layer of the design.

TABLE I  
DESIGN DIMENSIONS

Symbol	Value (mm)	Symbol	Value (mm)
$H1$	0.33	$WL$	1.85
$H2$	1.09	$Ws$	1
$H3$	10	$Ls$	11.65
$Wq$	5	$Wa$	3
$Lq$	18.5	$La$	26
$Ld$	16		

piece of solar cell placed in the center. Since the design isolates the effect of layer 1 of the antenna, it can have any shape or dimension as long as it does not intersect/overlap with a slot on layer 2. The design dimensions of our preliminary prototype operating around 2.4 GHz are listed in Table I. To host a  $60 \times 60 \text{ mm}^2$  solar panel, an overall board dimension of  $72 \times 72 \text{ mm}^2$  is chosen. Ideally, a smaller board dimension of  $66 \times 66 \text{ mm}^2$  can be used without overlapping the 3-mm slot width,  $W_a$ , on each side, but additional space is added to leave room for fabrication error.

The RF power is divided equally among each of the four radiating slots that are located symmetrically across the center of the design. The four lines that branch out to feed the slots have  $50\text{-}\Omega$  intrinsic impedance for  $WL = 1.85 \text{ mm}$ . Two of them are combined into a  $25\text{-}\Omega$  line, which then combine at the center of the structure for a total intrinsic impedance of  $12.5 \text{ }\Omega$ . By connecting the center to a  $25\text{-}\Omega$  quarter-wave impedance transformer, the other end of the impedance transformer is converted back to  $50 \text{ }\Omega$  and fed by a standard SMA. High-impedance lines are not used because they are too narrow for accurate fabrication. This feeding network allows the slots to be fed with same phase and power.

Slot is chosen as the radiator because the electric fields generated are vertical to any ground underneath the structure. In image theory, vertically polarized electric field is less affected by the ground reflection in comparison to horizontally polarized ones. Most wired antennas have poor performance when placed near and parallel to a ground plane because the ground image effectively cancels their horizontally polarized electric field. Each slot is excited by a T-shaped stub fed from the center. Since the slot is located at the edge of the RF ground plane, it is difficult to terminate the feed line in a microstrip stub mode when no ground plane is present on the other side of the slot. The

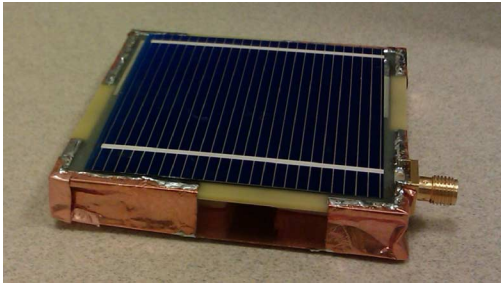


Fig. 4. Fabricated solar antenna prototype.

T-shaped stub does not need the signal line to propagate in microstrip mode after crossing the slot, thus it is desired for this design. The presence of the T-stub also makes the slot length,  $La$ , shorter than a half-wavelength with respect to the overall effective dielectric constant. Similar stub feeding can be found on some wideband slot antennas in the literature [25], [26]. The presented slot radiators are not wideband compared to the designs in literature because the proposed slots are narrower due to cavity height and the copper walls in the cavity eliminating blade-monopole-like ground resonances in the presented design. Other slot and feeding designs can also be considered to further improve the bandwidth.

The symmetrically placed slots dictate the radiation pattern of the antenna. Since each slot is fed in phase, the symmetry allows the four slots to launch a combined wavefront toward all four directions along the  $xy$  plane at the same time. Thus, the radiation pattern is close to omnidirectional.

The fabricated solar antenna prototype is shown in Fig. 4, with an overall size of  $72 \times 72 \times 11.5 \text{ mm}^3$ . A solar panel of  $60 \times 60 \text{ mm}^2$  is placed at the center of the structure without affecting the edge radiating elements. This means that 69% of the surface area is utilized by the solar cell. The dc power can reach inside the cavity with minimal RF interference by wiring along the cavity wall. This design can be easily scaled up to fit larger solar panels in order to provide more power to the wireless sensor node as long as the substrate loss is low enough for the feeding network to be effective.

### B. Simulation and Measurement

The antenna is simulated and tuned using CST Microstripes 2010 in free-space conditions. The solar cell is modeled as a  $60 \times 60 \text{ mm}^2$  copper plate, and it has little effect on the performance due to the presence of the  $72 \times 72 \text{ mm}^2$  RF ground plane. For the measurement, the antenna radiation and  $S_{11}$  is measured with and without the presence of a 50-cm-diameter ground plane in SATIMO's anechoic chamber as shown in Fig. 5. The measured and simulated  $S_{11}$  in Fig. 6 shows good agreement between the predicted and measured result. The lower measured frequency can be caused by the batch of FR4 having higher  $\epsilon_r$  than anticipated in the simulation.

The radiation pattern at 2380 MHz with and without a finite ground plane is shown in Fig. 7. The measurement results demonstrate that the antenna features an omnidirectional behavior comparable to a standard monopole [27] even in the presence of a ground plane. The measured gain is 0 dB in free-space condition and 4.4 dB above the ground plane. The measured ra-

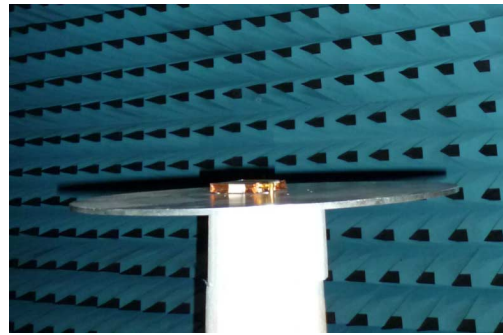


Fig. 5. Measurement setup of the antenna above a 50-cm-diameter ground plane.

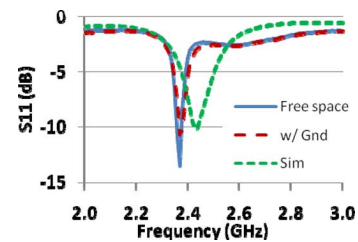


Fig. 6. Simulated and measured  $S_{11}$ .

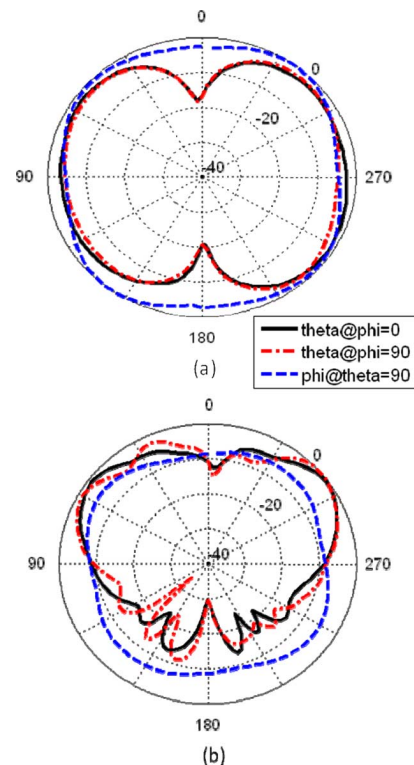


Fig. 7. Measured radiation pattern normalized (a) in free space and (b) placed above a 50-cm-diameter ground plane.

diation efficiency is 49% in free space and 52% with the ground plane at the operating frequency. The loss is mainly due to the dielectric loss of FR4 in the feeding network and the stub termination. Simulated efficiency improved from 50% to 99% when the FR4 loss is set to zero. The use of low-loss substrate between the RF signal and ground can significantly improve the radiation efficiency.

### III. CONCLUSION

A scalable low-profile omnidirectional antenna capable of integrating with a solar panel is presented. The antenna performance is comparable to a monopole antenna currently used in wireless sensor nodes. The antenna size can be easily modified to suit various solar panel sizes based on a sensor's power requirement. This work can enable self-sustainable ubiquitous sensors to be placed in "rugged" environments, such as roads, railways, rooftops, and vehicles.

### ACKNOWLEDGMENT

Any opinions, findings, and conclusions or recommendations expressed in this publication are those of the authors and do not necessarily reflect the view of the Federal Highway Administration.

The authors would like to thank Dr. A. Rohatgi for providing the solar cells, as well as K. Rutkowski and SATIMO Atlanta for the radiation measurement. The authors also appreciate inputs from Dr. L. Zhang and Dr. C. B. Theurer in GE Global Research.

### REFERENCES

- [1] F. Akyildiz, W. Su, Y. Sankarasubramaniam, and E. Cayirci, "A survey on sensor networks," *IEEE Commun. Mag.*, vol. 40, no. 8, pp. 102–114, Aug. 2002.
- [2] A. Sleman and R. Moeller, "Integration of wireless sensor network services into other home and industrial networks; Using Device Profile for Web Services (DPWS)," in *Proc. IEEE ICTTA*, 2008, pp. 1–5.
- [3] A. Hac, *Wireless Sensor Network Designs*. Hoboken, NJ: Wiley, 2003.
- [4] D. Malan, T. Fulford-Jones, M. Welsh, and S. Moulton, "CodeBlue: An ad hoc sensor network infrastructure for emergency medical care," presented at the MobiSys Workshop Appl. Mobile Embedded Syst., Jun. 2004.
- [5] "Huntington Botanical Gardens," SensorWare Systems, Pasadena, CA, 2003 [Online]. Available: [http://www.sensorwaresystems.com/historical/resources/huntington\\_sw31.shtml](http://www.sensorwaresystems.com/historical/resources/huntington_sw31.shtml)
- [6] "Solar powered wireless sensor networks monitor bridge spans," MicroStrain, Inc., Williston, VT, 2007.
- [7] D. M. Doolin and N. Sitar, "Wireless sensors for wildfire monitoring," in *Proc. SPIE Symp. Smart Structures Mater.*, San Diego, CA, Mar. 6–10, 2005, pp. 477–484.
- [8] "Prismark wireless technology report," Prismark, Cold Spring Harbor, NY, 2009.
- [9] M. Karpiriski, A. Senart, and V. Cahill, "Sensor networks for smart roads," in *Proc. IEEE Pervasive Comput. Commun. Workshops*, Mar. 2006, pp. 1–5.
- [10] H. Karl and A. Willig, *Protocols and Architecture for Wireless Sensor Networks*. Chichester, U.K.: Wiley, 2005.
- [11] D. Niyato, E. Hossain, and A. Fallahi, "Sleep and wakeup strategies in solar-powered wireless sensor/mesh networks: Performance analysis and optimization," *IEEE Trans. Mobile Comput.*, vol. 6, no. 2, pp. 221–236, Feb. 2007.
- [12] X. Jiang, J. Polastre, and D. Culler, "Perpetual environmentally powered sensor networks," in *Proc. IEEE Inf. Process. Sensor Netw. Symp.*, Apr. 2005, pp. 463–468.
- [13] "Chewed antennas: Huntington Botanical Gardens," SensorWare Systems, Pasadena, CA, 2003 [Online]. Available: <http://www.sensorwaresystems.com/historical/resources/pictures/hunt-011.shtml>
- [14] N. Henze, A. Giere, H. Fruchting, and P. Hofmann, "GPS patch antenna with photovoltaic solar cells for vehicular applications," in *Proc. IEEE VTC*, Oct. 2003, vol. 1, pp. 50–54.
- [15] J. Huang, "Mars rover antenna for solar-array integration," *Telecommun. Mission Oper. Prog. Rep.*, vol. 42–136, pp. 1–13, Oct.–Dec. 1998.
- [16] S. V. Shynu, M. J. R. Ons, M. J. Ammann, S. Gallagher, and B. Norton, "Inset-fed microstrip patch antenna with integrated polycrystalline photovoltaic solar cell," in *Proc. EuCAP*, Nov. 11–16, 2007, pp. 1–4.
- [17] N. Henze, M. Weitz, P. Hofmann, C. Bendel, J. Kirchhof, and H. Fruchting, "Investigation of planar antennas with photovoltaic solar cells for mobile communications," in *Proc. Person., Indoor Mobile Radio Commun.*, Sep. 5–8, 2004, vol. 1, pp. 622–626.
- [18] N. Nikolic, J. S. Kot, and T. S. Bird, "Theoretical and experimental study of a cavity-backed annular-slot antenna," *Proc. Inst. Elect. Eng., Microw., Antennas Propag.*, vol. 144, no. 5, pp. 337–340, Oct. 1997.
- [19] B. Jecko, "New kind of microstrip antenna: The monopolar wire-patch antenna," *Electron. Lett.*, vol. 30, no. 22, p. 1819, Oct. 1994.
- [20] E. Seeley, J. Burns, and K. Welton, "Cap-loaded folded antenna," in *IRE Int. Conv. Rec.*, Mar. 1958, vol. 6, pp. 133–138.
- [21] K. L. Lau and K. M. Luk, "A wide-band monopolar wire-patch antenna for indoor base station applications," *IEEE Antennas Wireless Propag. Lett.*, vol. 4, pp. 155–157, 2005.
- [22] H. Morishita, K. Hirasawa, and K. Fujimoto, "Analysis of a cavity-backed annular slot antenna with one point shorted," *IEEE Trans. Antennas Propag.*, vol. 39, no. 10, pp. 1472–1478, Oct. 1991.
- [23] S. Nikolaou, R. Bairavasubramanian, C. Lugo Jr., I. Carrasquillo, D. C. Thompson, G. E. Ponchak, J. Papapolymerou, and M. M. Tentzeris, "Pattern and frequency reconfigurable annular slot antenna using PIN diodes," *IEEE Trans. Antennas Propag.*, vol. 54, no. 2, pp. 439–448, Feb. 2006.
- [24] T. Wu, R. L. Li, and M. M. Tentzeris, "A mechanically stable, low profile, omni-directional solar-cell integrated antenna for outdoor wireless sensor nodes," in *Proc. IEEE APS*, Jun. 1–5, 2009, pp. 1–4.
- [25] F. Zhang, Q. Wu, and J.-C. Lee, "A simple T-shaped wide-band slot antenna for rectenna system," in *Proc. China–Japan Joint Microw. Conf.*, Sep. 10–12, 2008, pp. 444–446.
- [26] S. Chaimool, S. Kerdsomang, P. Akkraekthalin, and V. Vivek, "A broadband CPW-fed square slot antenna using loading metallic strips and a widened tuning stub," in *Proc. TENCON*, Nov. 2004, vol. C, pp. 539–542.
- [27] C. A. Balanis, *Antenna Theory: Analysis and Design*, 3rd ed. Hoboken, NJ: Wiley, 2005, pp. 721–726.